A numerical study on the pressure-reducing ability of DrainTube geosynthetics in an unsaturated embankment subject to rainfall

Michael G Andree, Ian R Fleming
Department of Civil, Geological, and Environmental Engineering – University of Saskatchewan, Saskatoon, SK, Canada
Stephan Fourmont
Afitex-Texel Geosynthetics Inc, Sainte-Marie, QC, Canada

ABSTRACT
This paper presents a finite element study on the application of a geosynthetic drainage product, DrainTube in an unsaturated embankment subject to rainfall. Materials used in the numerical study were characterized in terms of their unsaturated behavior. A pressure plate cell was used to obtain Water Characteristic Curves for two soils and the geosynthetic, and permeability of the geosynthetic was measured in a permeameter built specifically for geotextiles. Rainfall capture efficiency of the geosynthetic product was evaluated in a small-scale infiltration experiment, the results of which were also used to calibrate material parameters for the full numerical study. Various layouts and configurations of DrainTube were evaluated in an 3D numerical model with various rainfall rates using both calibrated soils. One such layout is discussed in this paper, and it is shown that implementing DrainTube offers a significant improvement over a geotextile-only solution.

RÉSUMÉ
Cet article présente une étude par éléments finis sur l'application d'un produit de drainage géosynthétique, le DrainTube, dans un remblai non saturé soumis aux précipitations. Les matériaux utilisés dans l'étude numérique ont été caractérisés en fonction de leur comportement non saturé. Une cellule à plaque de pression a été utilisée pour obtenir des courbes caractéristiques de l'eau pour deux sols et le géosynthétique, et la perméabilité du géosynthétique a été mesurée dans un perméamètre construit spécifiquement pour les géotextiles. L'efficacité de capture des précipitations du produit géosynthétique a été évaluée dans une expérience d'infiltration à petite échelle, dont les résultats ont également été utilisés pour calibrer les paramètres du matériau pour l'étude numérique complète. Différentes dispositions et configurations de DrainTube ont été évaluées dans un modèle numérique 3D avec différents taux de précipitations en utilisant les deux sols calibrés. Une telle disposition est discutée dans cet article, et il est démontré que la mise en œuvre de DrainTube offre une amélioration significative par rapport à une solution géotextile uniquement.

1 INTRODUCTION

There are a variety of drainage geosynthetics available and there is wide usage of geosynthetics in civil and environmental infrastructure. DrainTube is a drainage geosynthetic which incorporates a nonwoven geotextile that acts as a barrier and diversion blanket, and a small, perforated pipe that collects and moves fluid to a primary drain. Its uses have included leachate and landfill gas collection, drainage under foundations and sports fields, leak detection systems, among others. This paper will explore its application as a drain in a numerical model of an unsaturated reinforced embankment.

Characterization of the nonwoven geotextile component was explored in a prior paper by the authors (Andree and Fleming 2021) and included the Geotextile-Water Characteristic Curve (GWCC) and permeability function. Those characteristics are calibrated in a numerical model to an infiltration experiment and applied in the embankment scenario herein.

2 BACKGROUND

Iryo and Rowe (2005a) performed a numerical experiment for a sloping nonwoven geotextile and geonet in 2D to evaluate the diversion length that the geotextile would provide as a capillary barrier. They used a GWCC and permeability function that was consistent with that available in the literature. The mesh was made extremely fine in and directly above the geotextile region. They found that the diversion length was a function of infiltration rate, inclination, and pore air content and hypothesized that there would be a secondary diversion length related to flow from the geotextile entering the low air entry value (AEV) geonet.

PWRI (1988) constructed a small test embankment with geotextile reinforcement in various layouts. Capillary barriers were observed to develop as a result of the incompatible unsaturated properties of the geotextile and the sand with which the embankment was constructed. Failure of the embankment ultimately occurred due to the excess pore water that saturated the embankment face just above the geotextiles. These tests were modeled by Iryo

and Rowe (2005b) who expanded numerical seepage models into other geosynthetic layouts. They also performed stability analyses, for which the authors concluded that the geotextiles added much in the way of a reinforcing member than as a pressure-reducing drain.

Krisdani et al (2008) conducted infiltration experiments on a geonet sandwiched between two nonwoven geotextiles in a sand column. They started the experiment from an initially hydrostatic condition and allowed a drawdown to occur and a small capillary barrier to develop over a period of 48 hours. A rainfall rate of 5.8 mm/hr was then applied over a period of 6 hours and water storage above the geotextile was observed to increase significantly. Pressure rose to -0.2 m from the upper geosynthetic interface to the top of the column, but pressure below remained unchanged. Once infiltration was stopped for 72 hours, the pressure reduced near to the first drawdown condition. A numerical model was created to simulate the experiment, which approximated the physical model reasonably well.

Bathurst et al (2009) conducted an infiltration experiment in a sand-geotextile column. The experiment was run configured with a new geotextile in one iteration and a geotextile modified with a kaolin paste rubbed into the geosynthetic in another. The top boundary condition was a 0.1 m pressure head. Infiltration into the new geotextile developed a pore pressure of 0.05 m above the geotextile, while the modified geotextile developed a pore pressure over 0.5 m. Ponding at the soil-geosynthetic interface was not observed in other capillary barrier studies, which suggests that the top ponding boundary condition may produce a more severe effect.

Krisdani et al (2010) used an apparatus for soil capillary barrier testing (Tami et al 2004a, 2004b) to evaluate a geonet capillary barrier. They applied various rainfall rates and conducted a water balance on the flows at the downstream end. Water content increased above the geonet but remained unchanged below. All water was diverted above the geosynthetic, except in extreme rainfall conditions where a modest amount of water drained from the geonet.

Portelinha and Zornberg (2017) tested a fine-grained reinforced soil wall with 5 layers of nonwoven geotextiles under rainfall. Each layer acted as a barrier to flow for a period of 4 days before breakthrough occurred. Flow out of the geosynthetic was only observed once the water had permeated through each reinforcing layer. Displacements in the facing were observed as a result of the stored water prior to drainage.

These studies indicate that under unsaturated conditions, a geosynthetic intended as a drain may instead act as a barrier to drainage. This can be of practical use in some cases, but the usage of geosynthetics must be carefully examined for systems and climates where unsaturated conditions may exist.

3 MATERIALS

3.1 Characterized Geosynthetics

The geotextile-water characteristic curve (GWCC) was measured in a Tempe pressure plate apparatus over the drying phase. The apparatus was modified to include a plunger allowing for application of vertical confining pressure which also ensured contact between the geotextile and porous ceramic. Wetting curves were not obtained due to limitations of the apparatus.

Several variations of geotextile were tested, and results were similar despite their different thicknesses and densities of the fiber matrix. Figure 1 shows the GWCCs of one geotextile under several vertical loads. Figure 2 shows the GWCC of a second geotextile. The measured curves are consistent with those observed in the literature. Curve-fitting was conducted using the van Genuchten (1980) and Fredlund and Xing (1994) formulations, both of which provided a satisfactory fit.

The permeability function was measured with a custom-built permeameter which allowed for measurements of permeability at a variety of suctions. Andree and Fleming (2021) provide a full description of the experimental methods. Measured permeability plotted in Figure 3 is accompanied by the Fredlund, Xing and Huang (1994) permeability estimation which provided a good fit for the range of suctions tested.

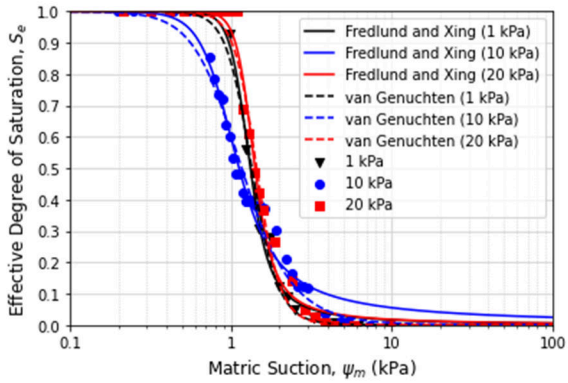

Figure 1. Geotextile 1 GWCC with Curve-fits under multiple vertical loads.

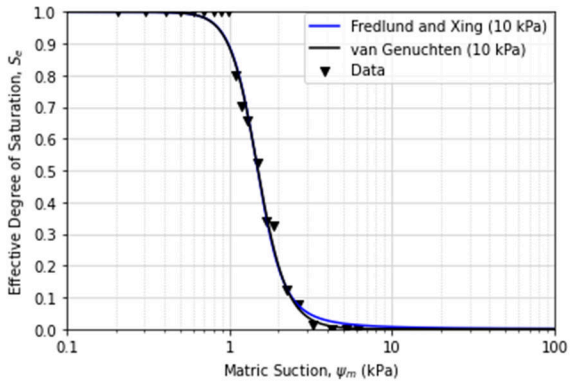

Figure 2. Geotextile 2 GWCC with Curve-fits under 10 kPa vertical load.

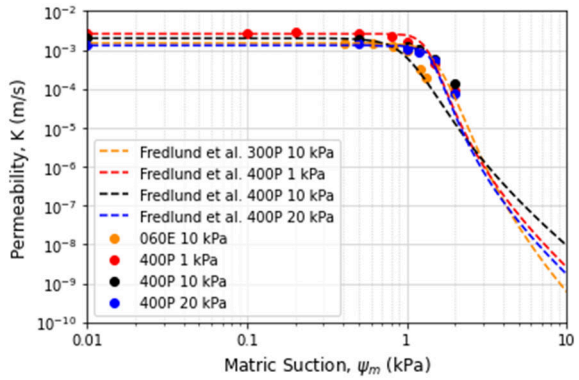

Figure 3. Geotextile Permeability Functions with Fredlund, Xing and Huang (1994) prediction

3.2 Characterized Soils

Two soil materials were selected. One was a commercially available aluminum oxide (alox) grit that is commonly used for sandblasting. The second material was a rock crusher dust that was sieved to a particle size of 75-150 microns with some fines present. Both soils are classified by USCS as silty sands. The grain size distributions (GSDs) of these materials are shown in Figure 4. The Soil-Water Characteristic Curves (SWCCs) in Figure 5 for both materials were measured in a Tempe pressure plate apparatus and curve-fitted. Fitting parameters for all materials are included in Table 1.

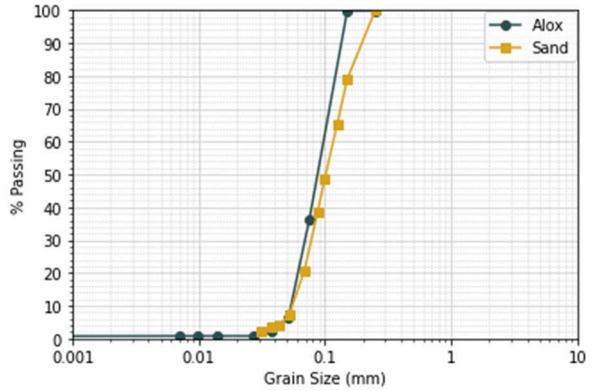

Figure 4. GSDs of Materials Used

4 INFILTRATION EXPERIMENT

4.1 Experimental Program

A series of infiltration experiments were undertaken to evaluate the effect the geosynthetic had on the pressure distribution under infiltration conditions in a column illustrated in Figure 6. The apparatus was constructed of PVC with a 20 cm x 20 cm cross section and stands 100 cm tall, with two 50 cm sections. The interior walls were lined with nonwoven geotextile to facilitate release of pore air during infiltration. The two sections were sealed prior to

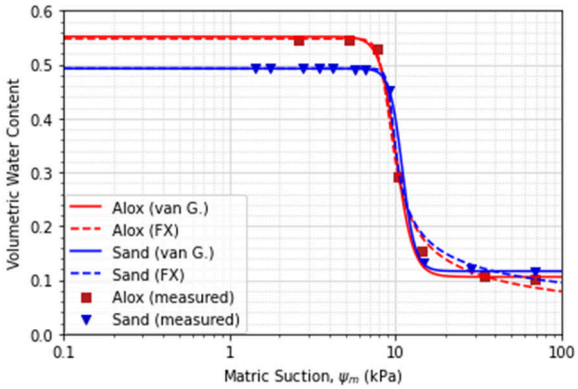

Figure 5. SWCCs of Alox and Sand

experiments with rubber matting and a commercially available viscous sealant.

A valve was installed 55 mm below the top of the lower section to facilitate drainage through the mini-pipe and was used as the datum. At the same elevation, a groove was cut into the apparatus wall and pinholes drilled through to facilitate drainage from the geotextile. Four METER Group Teros31 tensiometers were placed above the mini-pipe valve at 22 mm (two), 92 mm, and 144 mm and two were placed at 95 mm and 29 mm below. Tensiometers were logged with an Arduino-based system (Sattler et al 2020). Reference pressure was measured by a Barologger and logged with the Solinst Levelogger software.

The apparatus was filled by pluviating the soil material into the column as it filled with water. Once the soil reached the elevation of the geosynthetic, the geotextile was placed at the appropriate inclination and soil was placed to the column top. Infiltration was supplied by a peristaltic pump

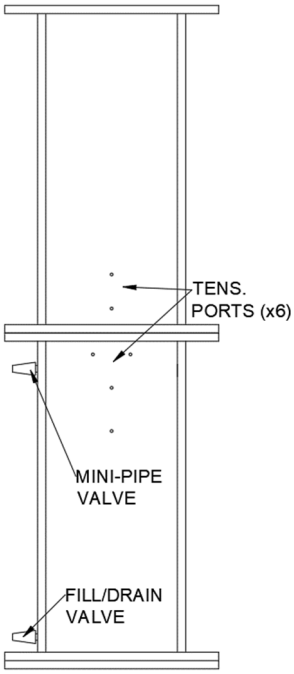

Figure 6. The Infiltration Column

Table 1. Curve-Fitting Parameters

Material (Vertical Load)	van Genuchten		Fredlund and Xing (1994)		
	a_{vg}	n_{vg}	a_{fx}	n_{fx}	m_{fx}
Geotextile 1 (1 kPa)	1.28	5.71	1.19	7.79	1.46
Geotextile 1 (10 kPa)	0.98	3.22	0.86	4.45	1.21
Geotextile 1 (20 kPa)	1.39	6.36	1.27	8.56	1.40
Geotextile 2 (10 kPa)	1.42	5.31	1.43	5.23	2.15
Aluminum Oxide Grit	9.96	8.98	8.28	14.81	0.64
Sand	10.90	11.72	9.14	24.61	0.40

which limited the lower bound of infiltration that could be applied. A 20 cm x 20 cm geotextile was placed on top of the soil column to facilitate spread of the water across the entire soil surface. The water table was set by a constant head tank connected to the bottom valve of the apparatus. The elevation of the tank was adjusted to change the water table level within the apparatus.

5 GEOSYNTHETIC CAPTURE

The geosynthetic capture was evaluated during the experiment. Rainfall rates from 15 mm/hr to 100 mm/hr were applied over the alox grit and 15 mm/hr to 140 mm/hr were applied to the sand. Capture was evaluated at water table elevations of 25 and 45 mm below the geosynthetic for both materials and additionally 220 mm for the sand.

The capture efficiency was found to be dependent chiefly on the infiltration rate and depth to the water table. As shown in Figure 7, the capture efficiency was higher when the water table is shallower. Interestingly, capture occurred with a water table at 220 mm below the geosynthetic in the sand but did not occur at similar conditions when applied over the alox grit.

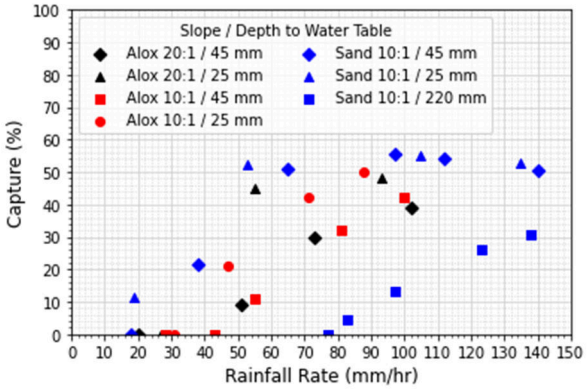

Figure 7. Total Geosynthetic Capture

It was not possible to evaluate the effect of geosynthetic inclination as there was no difference in capture observed between the 5% and 10% slope. This was believed to be a limitation of the apparatus scale.

6 CALIBRATION OF MATERIALS

A numerical model was constructed using GeoStudio SEEP3D with the same dimensions as the physical infiltration apparatus. A unique steady-state analysis was created for each rainfall rate and water table level that was experimentally tested. A transient analysis was not meaningful due to the high degree of saturation in the soil materials due to their high AEVs near 8 kPa. A coarser soil with a lower AEV such as that tested by Krisdani et al (2008) would have been suitable.

The geotextile was represented as a 3 mm thick prism with a 1 mm mesh. The soil near the geotextile was meshed similarly fine and became larger with distance from the geotextile. The mini-pipe was represented as “seepage face” boundary condition, which requires the program to review the nodes along the boundary to check for positive pressures. If pressures are above 0 kPa, the node is set to a zero-pressure boundary condition. The downstream end of the geotextile was also represented by this condition.

Since a wetting characterization could not be experimentally obtained in the prior research, the GWCC and permeability function from Iryo and Rowe (2005a) were adopted and produced satisfactory numerical results. The authors deem this substitution acceptable due to the similarities in these curves for unsaturated of nonwoven geotextiles demonstrated in the literature.

Calibration was achieved simply by adjusting the saturated permeability of the geotextile, alox grit, and sand. The calibrated WCCs and permeability functions are shown in Figures 8 and 9. These characteristic functions were also slightly “softened” by changing the fitting parameters to ease the transition between saturated, desaturation, and residual states which enhances the solver’s ability to converge while not significantly altering the characteristics of the material.

7 MODEL EMBANKMENT

7.1 Model Description

Transient 3D models were constructed in SEEP3D based on the 3 m tall embankment model by Iryo and Rowe (2005b). Analyses had durations of several days to achieve a steady-state pressure condition. The model geometry is illustrated in Figure 10 and the boundary conditions are

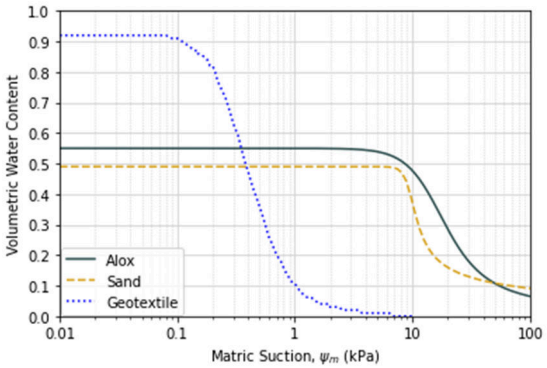

Figure 8. Calibrated WCCs

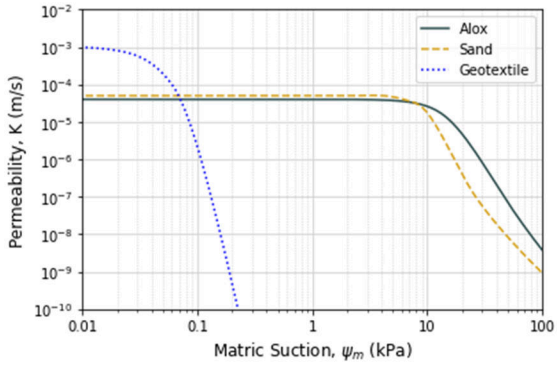

Figure 9. Calibrated Permeability Functions

described in Table 2. A screenshot of the SEEP3D model is presented in Figure 11. Materials calibrated in the numerical infiltration model were used. No consideration for stability was made, however it should be noted that a physical test embankment constructed by PWRI (1988) on which Iryo and Rowe (2005b) based their model failed due

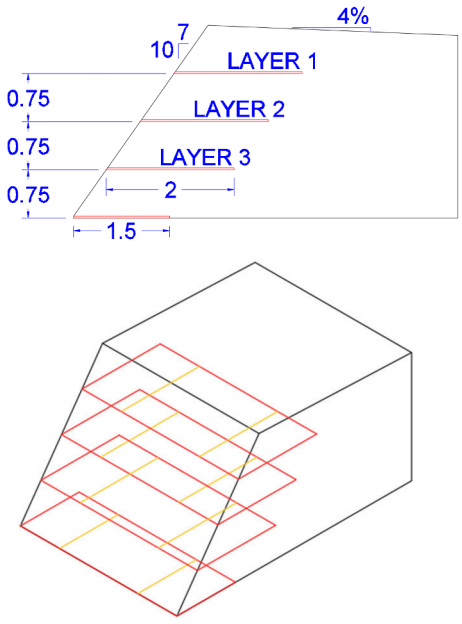

Figure 10: Embankment Model Geometry

Table 2. Embankment Model Boundary Conditions

Boundary	Boundary Condition	Notes
Lateral Extents, Back, Bottom	No-Flow	-
Top	Flux Rate (m/s)	Rainfall Rate
Slope Face	Flux Rate (m/s) with Seepage Face	Rainfall Rate (adjusted for slope)
Geotextile ends at Slope Face	Flux Rate (m/s) with Seepage Face	Rainfall Rate (adjusted for slope)
Mini-Pipe	Seepage Face	0 m upon review

to saturated of the soil above the geosynthetic due to capillary break development. The same geotextile layouts were used with the incorporation of the mini-pipes spaced at 0.25, 0.5, 1, and 2 m to evaluate the effect of spacing on performance. Results from one of the geosynthetic layouts is presented in this paper.

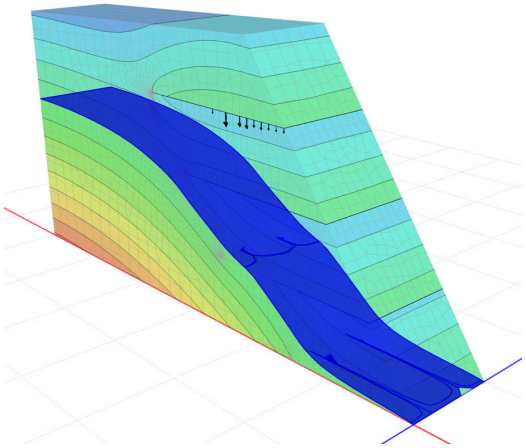

Figure 11. Screen capture from SEEP3D Model

7.2 Vertical Pressure Profiles

Vertical profiles presented in Figures 12 and 13 below illustrate the effect of the geotextile and mini-pipe on the hydraulic conditions within the sand embankment under rainfall conditions of 12.7 mm/hr and 36 mm/hr. A clear capillary barrier develops at the geotextile interface with greater severity at the upper elevations, exceeding the base case pressure. The geosynthetic-only case provided little reduction in pressure head over the base case over the full profile, while the inclusion of mini-pipes provided relief of pore pressure, particularly between elevations 0 m and 0.75 m. It is also evident that a tighter spacing of mini-pipes provides a greater reduction in pressure head, particularly at the embankment toe.

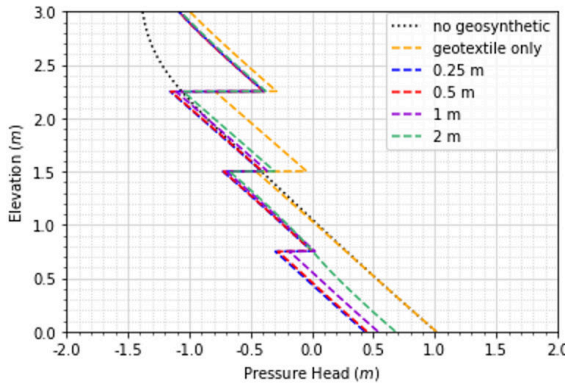

Figure 12. Profile for rainfall of 12.7 mm/hr

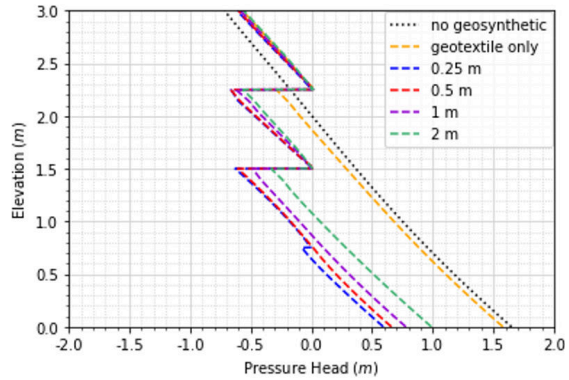

Figure 13. Profile for rainfall of 36 mm/hr

7.3 Relationship between h_p and K_{sat}/q

Figures 14-17 illustrates the relationship between peak pressure head and infiltration expressed as K_{sat}/q. The clear reduction in pore pressure at 0 m is again seen in Figure 14 where pressure head at all rainfall rates are below the base case. A similar conclusion can be made for Figure 15 at the top of the interface at 0.75 m where pressures remained less than the base case.

At the mid-slope elevation of 1.5 m, the relationship becomes more complex. Figure 16 shows a reduction in pressure head by all drain spacings for K_{sat}/q approximately less than 8 (shown in blue), but pressure heads for spacings 1 m and 2 m were in excess of the base case for K_{sat}/q approximately greater than 8 (in red). In Figure 17 at elevation 2.25 m, pressure head exceeded the base case for all spacings and all rainfall rates due to the proximity to the infiltration source. Pressure head peaks slightly above zero for K_{sat}/q approximately up to 8 but decreases below zero beyond that point.

8 CONCLUSIONS

An infiltration experiment was conducted to evaluate the capture efficiency of DrainTube. The experimental GWCC and permeability of the geotextile were calibrated in a 3D numerical model of the infiltration experiment. The

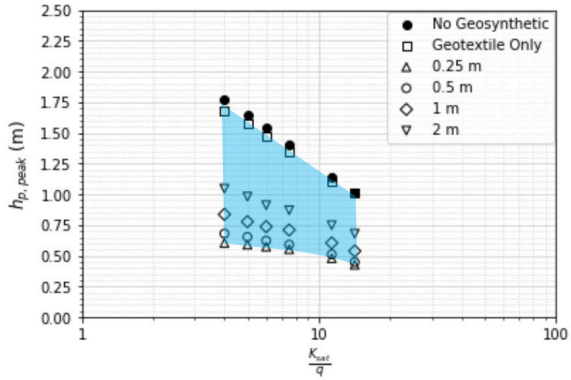

Figure 14. Peak h_p as a function of K_{sat}/q at 0 m

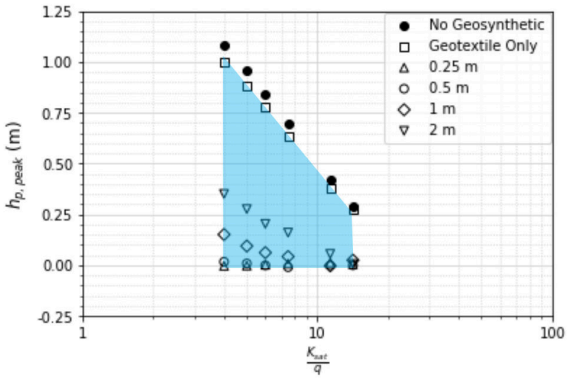

Figure 15. Peak h_p as a function of K_{sat}/q at 0.75 m

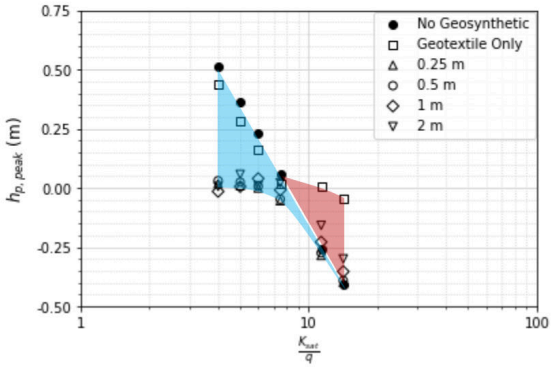

Figure 16. Peak h_p as a function of K_{sat}/q at 1.5 m

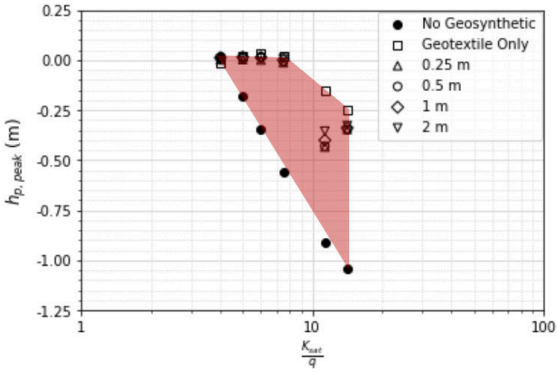

Figure 17. Peak h_p as a function of K_{sat}/q at 2.25 m

calibrated materials were then used in an embankment drainage scenario.

A geotextile-only drain provided little benefit over the base case and was in fact the cause of failure in the prior physical study by PWRI (1988). The introduction of mini-pipes in the numerical model provided a reduction in pressure head within the embankment, especially at the toe. Pressure head was higher than the base case at intermediate elevations, though generally below 0 m. It was evident that a tighter mini-pipe spacing provided further relief of pressure.

9 ACKNOWLEDGEMENTS

Funding and support for this research was provided by Afitex-Texel Inc., Groupe CTT, and Mitacs.

10 REFERENCES

Andree, MG and Fleming, IR. 2021. Unsaturated Characterization and Permeability of a Nonwoven Geotextile. *GeoNiagara 2021*, Niagara, ON.

Bathurst, RJ, Siemens, G, and Ho, AF. 2009. Experimental investigation of infiltration ponding in one-dimensional sand-geotextile columns. Geosynthetics International, 16(3): 158–172.

Fredlund, DG, and Xing, A. 1994. Equations for the soil-water characteristic curve. *Canadian Geotechnical Journal* 31(4): 521-532.

Fredlund, DG, Xing, A, and Huang, S. 1994. Predicting the permeability function for unsaturated soils using the soil-water characteristic curve. *Canadian Geotechnical Journal* 31(4): 533-546.

van Genuchten, M.T. 1980. A Closed-form Equation for Predicting the Hydraulic Conductivity of Unsaturated Soils. *Soil Science Society of America Journal*, 44(5): 892–898.

Iryo, T and Rowe, RK. 2005a. Hydraulic behaviour of soil-geocomposite layers in slopes. *Geosynthetics International*, 12(3): 145–155.

Iryo, T, and Rowe, RK. 2005b. Infiltration into an embankment reinforced by nonwoven geotextiles. *Canadian Geotechnical Journal*, 42(4): 1145–1159.

Krisdani, H, Rahardjo, H, and Leong, E-C. 2008. Measurement of geotextile-water characteristic curve using capillary rise principle. *Geosynthetics International*, 15(2): 86–94.

Krisdani, H, Rahardjo, H, and Leong, E-C. 2010. Application of geosynthetic material in capillary barriers for slope stabilisation. *Geosynthetics International*, 17(5): 323–331.

Portelinha, FHM, and Zornberg, JG. 2017. Effect of infiltration on the performance of an unsaturated geotextile-reinforced soil wall. *Geotextiles and Geomembranes*, 45(3): 211–226.

PWRI, Toyobo Co. Ltd., Toray Industries Inc., and Unitika Ltd. 1988. Development of Reinforcing Method for Embankment Using Spunbond Nonwoven Geotextile. Performance of Geotextile Within Soil and Its Effectiveness, Vol. 2, Cooperative research report of PWRI, No. 6. Tsukuba, Japan.

Sattler, KD, Elwood, D, Hendry, MT, Berscheid, B, Marcotte, B, Haji Abdulrazagh, P, and Huntley, D. 2020. Open source software for data collection from SDI-12 sensors connected to an Arduino microcontroller. University of Alberta. Edmonton, AB.

Tami, D, Rahardjo, H, Leong, E-C, and Fredlund, DG. 2004a. A Physical Model for Sloping Capillary Barriers. *Geotechnical Testing Journal*, 27(2): 173–183.

Tami, D, Rahardjo, H, Leong, E-C, and Fredlund, DG. 2004b. Design and laboratory verification of a physical model of sloping capillary barrier. *Canadian Geotechnical Journal*, 41: 814–830.